HHS Public Access

Author manuscript

Cell Rep. Author manuscript; available in PMC 2022 June 13.

Published in final edited form as:

Cell Rep. 2022 May 24; 39(8): 110843. doi:10.1016/j.celrep.2022.110843.

A nickase Cas9 gene-drive system promotes super-Mendelian inheritance in *Drosophila*

Víctor López Del Amo[1,2,*], **Sara Sanz Juste**[1], **Valentino M. Gantz**[1,*]

[1]Section of Cell and Developmental Biology, University of California, San Diego, La Jolla, CA 92093, USA

[2]Lead contact

SUMMARY

CRISPR-based gene-drives have been proposed for managing insect populations, including disease-transmitting mosquitoes, due to their ability to bias their inheritance toward super-Mendelian rates (>50%). Current technologies use a Cas9 that introduces DNA double-strand breaks into the opposing wild-type allele to replace it with a copy of the gene-drive allele via DNA homology-directed repair. However, the use of different Cas9 versions is unexplored, and alternative approaches could increase the available toolkit for gene-drive designs. Here, we report a gene-drive that relies on Cas9 nickases that generate staggered paired nicks in DNA to propagate the engineered gene-drive cassette. We show that generating 5′ overhangs in the system yields efficient allelic conversion. The nickase gene-drive arrangement produces large, stereotyped deletions that are advantageous to eliminate viable animals carrying small mutations when targeting essential genes. Our nickase approach should expand the repertoire for gene-drive arrangements aimed at applications in mosquitoes and beyond.

In brief

Gene-drives using wild-type Cas9 offer solutions to fight vector-borne diseases, yet alternative strategies are needed to increase the available toolkit. López Del Amo et al. describe a nickase-based gene-drive system that promotes super-Mendelian inheritance of an engineered cassette in the *Drosophila* germ line, providing alternative designs for CRISPR-based gene-drive.

Graphical Abstract

*Correspondence: vlopezdelamo@ucsd.edu (V.L.D.A.), vgantz@ucsd.edu (V.M.G.).

AUTHOR CONTRIBUTIONS

V.L.D.A. and V.M.G. conceived the project. V.L.D.A. designed and obtained the nickase gene-drive constructs in *Drosophila*. V.L.D.A. and S.S.J. performed the experiments. V.L.D.A., V.M.G., and S.S.J. created the figure visualizations. V.L.D.A. wrote the manuscript, which was edited by all of the authors.

DECLARATION OF INTERESTS

V.M.G. has equity interests in Synbal and Agragene, companies that may benefit from the research results, and serves on both companies' Scientific Advisory Boards and on the Board of Directors of Synbal. The terms of this arrangement have been reviewed and approved by the University of California, San Diego in accordance with its conflict-of-interest policies.

SUPPLEMENTAL INFORMATION

Supplemental information can be found online at https://doi.org/10.1016/j.celrep.2022.110843.

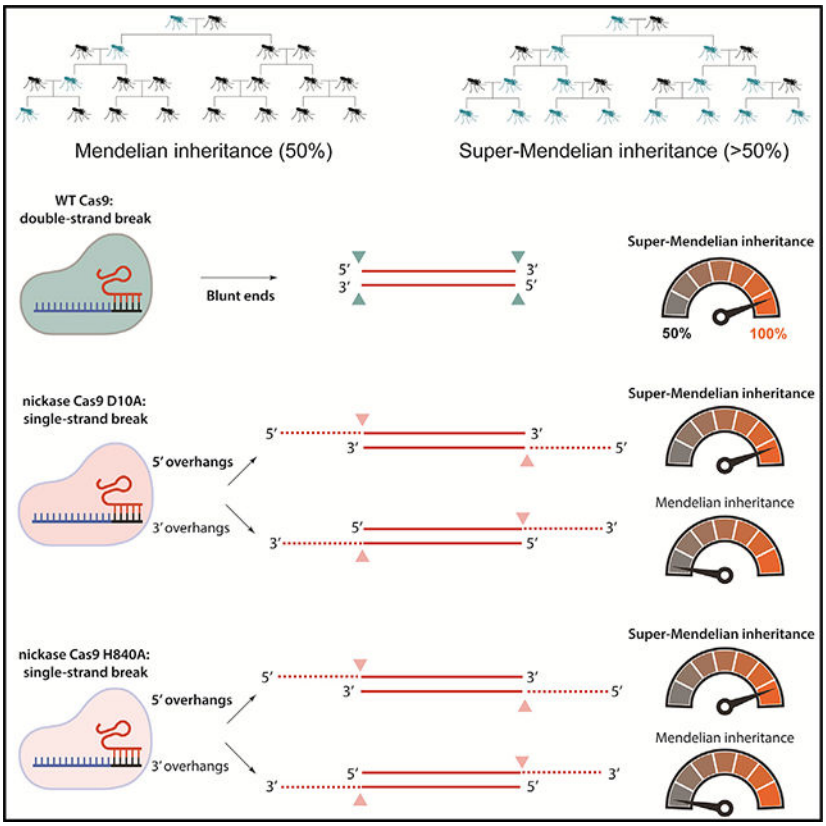

INTRODUCTION

CRISPR gene-drive systems have emerged as a promising tool for disseminating engineered traits into wild populations to control disease transmission. This rapid dissemination is possible due to the ability of these systems to surpass Mendel's first law of gene segregation, which dictates that an allele has a 50% probability of being passed to the next generation; in fact, gene drives can reach up to 100% inheritance of a desired allele. A proof-of-concept system was first implemented in flies (Gantz and Bier, 2015) and was applied to different mosquitoes such as *Anopheles* or *Aedes* under laboratory conditions to fight vector-borne diseases (Adolfi et al., 2020; Gantz et al., 2015; Hammond et al., 2016; Kyrou et al., 2018; Li et al., 2020; Simoni et al., 2020).

CRISPR-based gene-drives consist of a three-component transgene: (1) Cas9, a DNA nuclease that produces DNA double-strand breaks; (2) a guide RNA (gRNA) that directs Cas9 to cleave the DNA at a predetermined site; and (3) two homology arms flanking the Cas9/gRNA components that perfectly match both sides of the cut site to promote homology-directed repair (HDR). When a gene-drive individual mates with a wild-type, the encoded Cas9 from the engineered gene drive cuts the wild-type allele in the germ line, which is replaced by HDR using the intact gene-drive chromosome as a repair template. With the gene-drive present on both alleles (i.e., homozygous), this process produces a super-Mendelian inheritance (>50%) of the engineered cassette to spread new traits through a population. Current gene-drive methods use a Cas9 that introduces DNA double-strand

breaks (Adolfi et al., 2020; Bier, 2021; Gantz et al., 2015; Hammond et al., 2016; Kyrou et al., 2018; Li et al., 2020; Simoni et al., 2020). However, we lack alternative Cas9-based strategies that could enlarge the available toolkit for gene-drive designs while potentially bringing advantages to improve the current ones. In fact, mutant versions of Cas9 that only generate nicks should also be amenable. Wild-type Cas9 contains two endonuclease domains (HNH and RuvC-like domains) that can introduce DNA double-strand breaks, in which each cleaves one strand of the DNA double-helix (Gasiunas et al., 2012; Jinek et al., 2012). By mutating critical residues in the nuclease domains, two nickase versions of Cas9 can be generated: (1) nCas9-D10A (nD10A) contains an inactivated RuvC domain and only cuts the target strand where the gRNA is bound, and (2) nCas9-H840A (nH840A) contains an inactivated HNH and thus only cuts the non-target strand (Gasiunas et al., 2012; Jinek et al., 2012).

Importantly, the nickase versions of Cas9 already demonstrated their efficiency for genome editing. nD10A has been used to generate paired DNA nicks and efficiently disrupts genes in *Drosophila* and cell culture (Gopalappa et al., 2018; Port et al., 2014). Nicks induced by nD10A promoted higher HDR rates than nH840A, in which HDR was almost undetectable (Bothmer et al., 2017; Hyodo et al., 2020; Mali et al., 2013; Wang et al., 2018, 2021). Furthermore, nD10A can boost specificity while reducing off-target effects since it requires two gRNAs that target complementary DNA strands to either disrupt a gene function or trigger HDR. When the same pair of gRNAs were combined with wild-type Cas9, undesired off-target effects at an unspecific genomic region were generated, which does not occur with nD10A (Ran et al., 2013).

Nickase Cas9 (nCas9) versions have been extensively used *in vitro* to evaluate HDR efficiencies. However, only a few studies attempted to use nickase-based approaches of paired-gRNAs using mice and *Drosophila*, in which nD10A promoted modest HDR rates (Lee and Lloyd, 2014; Ren et al., 2014). Therefore, the design of novel strategies using both nD10A and nH840A to induce meaningful HDR rates in the germ line of a living organism is needed to better understand the fine workings of nickase-based HDR *in vivo*. We reasoned that a nCas9-based gene-drive may be applicable for population engineering to bring potential advantages. For example, DNA nicks are involved in important biological processes such as DNA replication and are typically repaired efficiently (Caldecott, 2008; Chafin et al., 2000; Reyes et al., 2021; Wang and Hays, 2007). Therefore, if paired nicks do not occur simultaneously, single nicks could restore the original wild-type sequence, reducing the formation of mutations or resistant alleles at the target site, and allowing further gene-drive conversion. In addition, DNA nicks follow distinct DNA repair pathways compared to DNA double-strand breaks that are introduced by traditional gene drives (Vriend and Krawczyk, 2017), and the intrinsically offset distance between paired nicks in a gene-drive setting could favor the formation of specific mutations to improve gene-drive propagation in certain applications.

Thus, we envisioned that simultaneous paired nicks targeting two adjacent DNA regions should generate a staggered double-strand break followed by DNA repair by HDR to promote super-Mendelian inheritance of an engineered gene-drive construct. Here, we developed an nCas9-based gene-drive system promoting super-Mendelian inheritance in

Drosophila melanogaster as a proof-of-concept and showed that nD10A and nH840A can promote efficient HDR in the germ line. Interestingly, we showed that super-Mendelian inheritance rates can be achieved only when the gene-drive design generated 5′ overhangs. We also showed that nH840A produces larger deletions compared to nD10A when the allelic conversion fails. This feature can be used to reduce the presence of viable animals carrying small mutations when targeting essential genes, as we could design strategies to generate large deletions removing critical protein domains to ensure the lethality of insects. Overall, this work expands the technology and applicability of CRISPR gene-drive systems for genetic engineering of wild populations.

RESULTS

Nickase gene-drive system can be tailored to induce 5′ or 3′ overhangs

To design a nickase-based gene-drive, we used a gRNA-only split-drive system (i.e., Copycat) that consists of two separate components: (1) a transgenic fly carrying a static Cas9 transgene, which is inherited in a Mendelian fashion, and (2) an engineered animal carrying a CopyCat cassette formed by a gRNA gene that is flanked by two homology arms (Gantz and Bier, 2016). Once the two components are genetically crossed, traditional CopyCat gene-drives rely on DNA double-strand breaks produced by a single gRNA, which targets the same sequence on the wild-type allele where it is inserted, to propagate the synthetic cassette by HDR (Champer et al., 2019; Gantz and Bier, 2016; López Del Amo et al., 2020a; Xu et al., 2017) (Figure 1A). In contrast, our nickase-based gene-drive system requires two gRNAs since this modified Cas9 introduces nicks instead of double-strand breaks. In this case, the gRNA pair will produce two independent cleavage events on each of the complementary DNA strands for gene-drive propagation by HDR, emulating traditional gene-drives (Figure 1B).

To build a gene-drive system based on an nCas9, we generated two transgenic lines containing a DsRed marker and carrying either the nD10A or nH840A versions, which cut the target strand (bound to the gRNA) or the non-target strand, respectively. In addition, we used a validated wild-type Cas9 line, which introduces DNA double-strand breaks (López Del Amo et al., 2020b) as a positive control (Figure 1C). We inserted all Cas9 transgenes into the *yellow* locus and expressed them with the same *vasa* germline promoter. Separately, we built two Copycat gene-drive constructs that we inserted into the *white* gene to produce two distinct gRNAs. To ensure perfect homology and a proper HDR process, the two homology arms included as part of the CopyCat elements match each cut site of the gRNA pair. We used a GFP marker to track the inheritance of these transgenes. Both Copycat lines share the *w2*-gRNA, which we previously validated (López Del Amo et al., 2020a, 2020b), and were combined with either the *w8*-gRNA or the *w9*-gRNA as the second gRNA (Figure 1D). In addition, protospacer adjacent motif (PAM) DNA sequences are crucial for target location recognition (Jinek et al., 2012), and these constructs present different PAM orientations depending on the gene-drive element. The Copycat transgenic line containing *w2,w8*-gRNAs pairs (CC(*w2,w8*)) have PAMs that face in opposite directions (i.e., a PAM-out orientation). In contrast, the transgenic strain carrying the *w2,w9*-gRNAs pairs (CC(*w2,w9*)) have PAMs that face each other (i.e., a PAM-in orientation). All three gRNAs

are located within an ~100-bp DNA window, and the paired gRNA cut sites are separated by approximately 50 nt (Figure 1D).

We combined the nickases with the two CopyCat transgenic lines to create four schemes to test the nickase gene-drive system: (1) nD10A with the CC(*w2,w9*) (PAM-in) to generate 3′ overhangs; (2) nD10A with the CC(*w2,w8*) (PAM-out) to generate 5′ overhangs; (3) nH840A with CC(*w2,w9*) (PAM-in) to generate 5′ overhangs; and (4) nH840A with the CC(*w2,w8*) (PAM-out) transgenic line to generate 3′ overhangs. Importantly, combining either of the CopyCat lines with wild-type Cas9 produces similar blunt ends in both situations (Figure 1E).

Cas9 nickases promote super-Mendelian inheritance of the Copycat gene-drive elements

To evaluate the efficiency of our CopyCat elements, we used the same genetic cross-scheme in all cases. We combined male flies containing the Cas9 source (wild-type Cas9, nD10A, or nH840A) with the CopyCat lines to obtain F_1 trans-heterozygous animals carrying both transgenes. We then crossed these F_1 females to a white mutant line to evaluate biased inheritance in their F_2 progeny. If the Copycat is inactive, then we should observe 50% inheritance of the GFP marker, which is integrated within the engineered cassette as mentioned. If the CopyCat construct can promote HDR in the germline, it should display super-Mendelian inheritance (>50%) of the GFP-marked transgene. All Cas9 sources, which carry the dsRed marker, should have ~50% inheritance (Figure 2A).

When combining the wild-type Cas9 with both CopyCat elements, we introduce two proximal DNA double-strand breaks by a multiplexing approach (Figure 1E), which efficiently biases Mendelian inheritance (Champer et al., 2018). Here, we observed similar super-Mendelian inheritance levels of ~97% with both PAM-out and PAM-in CopyCat elements (Figure 2B). We did not observe significant differences between CopyCat elements when combined with the wild-type Cas9 ($p = 0.6721$, see statistics in Data S1), suggesting that both gRNA combination pairs would have similar efficiencies as a unit. In our previous work, we individually validated the *w2*-gRNA in a similar CopyCat arrangement that showed 90% super-Mendelian inheritance (López Del Amo et al., 2020a). Here, adding a second gRNA (*w8* or *w9*) boosted the allelic conversion efficiency from 90% to ~97% in both cases. While these results concur with reports of increased gene-drive performance with an additional gRNA (Champer et al., 2018), we cannot determine the contribution of each gRNA singularly in a multiplexing approach due to different cleavage window activities and PAM orientations between gRNA pairs.

After confirming the activity of the two elements built to test the nickase gene drive, we evaluated the ability of nCas9 to promote super-Mendelian inheritance in either of the four defined scenarios (Figure 1E). We crossed our nD10A transgenic line with both CopyCat strains carrying the tandem gRNAs and followed the same experimental cross-scheme (Figure 2A). In this case, the nD10A version displayed 93% super-Mendelian inheritance levels when combined with the CC(*w2, w8*) that generated 5′ overhangs. In contrast, the CC(*w2, w9*) (PAM-in) that generated 3′ overhangs was inherited in a Mendelian fashion (~50%) (Figure 2C; Data S2).

We also tested the nH840A line following the same cross-scheme (Figure 2A). nH840A produced super-Mendelian inheritance rates of ~85% when combined with the CC(*w2, w9*) (PAM-in) that generated 5′ overhangs. However, we observed 50% inheritance rates when combined with the CC(*w2, w8*) (PAM-out) to generate 3′ overhangs (Figure 2C; Data S2). Interestingly, we observed super-Mendelian inheritance when using both nD10A and nH840A, yet nD10A produced biased inheritance only when combined with the CC(*w2, w8*), while nH840A triggered super-Mendelian inheritance when crossed to the CC(*w2, w9*). Therefore, we detected gene-drive activity only when 5′ overhangs were generated, and these results concurred with previous *in vitro* studies in which paired nicks only stimulated significant HDR levels when using nD10A to generate 5′ overhangs (Mali et al., 2013; Ran et al., 2013).

Overall, nD10A performed significantly better than nH840A for inheritance bias when generating 50 overhangs ($p < 0.0001$, see statistics in Data S2), which could be due to different cleavage rates between the nickases. Since the *white* gene targeted for conversion in our system is tightly linked with the *yellow* gene where all of our Cas9 sources are inserted, our experimental design allowed us to evaluate conversion (HDR), mutations (resistant alleles), and wild-type/uncut allele rates arising from all of the conditions tested via the F_2 progeny (Figure S1). nD10A displayed 95% cutting efficiency, which is higher than nH840A that showed 91% cutting rates ($p = 0.0683$; see statistics in Data S1; Figure S1) We also observed that nD10A displayed higher conversion rates (85%) compared to the nH840A (70%). Most important, nickases producing biased inheritance contained ~5–10% wild-type alleles, suggesting that DNA nicks can restore the original wild-type sequence to allow further gene-drive conversion (Figure S1).

Altogether, we have demonstrated the example of a gene-drive system driven by an nCas9, which simultaneously nicks both complementary strands to induce efficient allelic conversion that is mediated by HDR *in vivo*. Furthermore, our data indicate that super-Mendelian inheritance through nickase gene drives can be achieved only by generating 5′ overhangs.

DNA double-strand breaks introduced by gene-drives can produce resistant alleles at the target site when the HDR-mediated allelic conversion process is inaccurate. Resistant alleles generated by wild-type Cas9 have been characterized by us and other groups (Champer et al., 2018; Gantz and Bier, 2015; Hammond et al., 2017; López Del Amo et al., 2020b). However, the types of resistant alleles generated by paired nicks are uncharacterized in a gene-drive context. Here, we identified and evaluated the resistant alleles generated by our wild-type Cas9 and nickase gene-drive systems that promoted super-Mendelian inheritance (Figures 2B and 2C). Since the CopyCat target is the *white* gene located in the X chromosome, and males have only one X chromosome, GFP^- F_2 males that present the *white* eye phenotype indicate *white* gene disruption and unsuccessful allelic conversion, indicating individuals that carry resistant alleles.

We extracted the DNA from these animals and characterized them by Sanger sequencing. We observed five different classes of resistant alleles: (1) large deletions spanning both cut sites (>50 bp), (2) deletions (<50 bp) occurring at one cut site with the other cut

site intact, (3) simultaneous deletions (<50 bp) at both target sites with partial sequence retention between cut sites, (4) large insertions (>200 bp), and (5) small insertions combined with small deletions in the same individuals at the same cut site (i.e., insertion + deletion) (Figures 2D and S2).

When we sequenced F_2 flies arising from the nH840A and PAM-in gRNAs combination that carried resistant alleles, we detected that 42% of these individuals contained large deletions spanning 50–90 nt (Figures 2E and S2A). This is a significantly higher frequency of large deletions spanning both nick sites compared to the nD10A PAM-out (5%) (Figure 2E; $p = 0.0389$, see statistics in Data S3). Similarly, wild-type Cas9 combined with PAM-out and PAM-in gRNAs displayed a lower percentage of large deletions, ~5% and ~20%, respectively, compared to the nH840A PAM-in combination (Figure 2E; Data S3).

We also observed large insertions (>200 bp) when nD10A was combined with paired gRNAs in a PAM-out orientation (Figure S2D). We found that 25% of the sequenced flies within this condition had large insertions, which was significantly higher than nH840A combined with PAM-in gRNAs, where we did not detect any large insertion event (Figure 2E; $p = 0.0143$, see statistics in Data S3). In line with these observations, the wild-type Cas9 only produced large insertions when combined with the PAM-out gRNAs, suggesting that PAM orientation can influence resistant allele outcomes (Figure 2E; Data S3). The large insertions produced by the PAM-out gRNAs represented partial HDR occurrences containing portions of the engineered gene-drive allele. We detected either part of the U6 promoter downstream of the left homology arm or the synthetic 3xP3 promoter with an incomplete piece of the GFP marker downstream of the right homology arm of the gene-drive element (Figure S2D). While previous gene-drive studies showed the formation of insertions with either a multiplexing approach (Champer et al., 2018) or traditional gene-drives with a single gRNA (Hammond et al., 2017), this outcome seems to be a more prominent phenomenon of the PAM-out arrangement in our work.

We did not observe significant differences between the nickase genotypes in the other categories described above, including single cuts at only one target site, simultaneous mutations at both cut sites, or insertion + deletion events happening in the same individual (Figures 2D and 2E; see statistics in Data S3). However, it is noteworthy that we observed a significant percentage of simultaneous small mutations occurring at both cut sites when using wild-type Cas9 with PAM-out and PAM-in gRNAs, 25% and 72%, respectively. Interestingly, these occurrences were almost undetectable when our gene-drive elements were combined with nickases (Figure 2E; see statistics in Data S3). Instead, both nickases presented higher rates of resistant alleles containing mutations at only one target site at a time (Figure 2E). This may indicate that DNA double-strand breaks induce small deletions if allelic conversion fails while DNA nicks can restore the wild-type sequence. Indeed, this aligns with the presence of wild-type alleles (uncut) when using nickase versions of Cas9 (Figure S1).

Overall, we confirmed that the gRNAs in this work are active, as we found mutations at all target sites within the genotypes that produced super-Mendelian inheritance (Figure S2). In

addition, we have shown different repair outcomes when using distinct Cas9 sources, which can inform future gene-drive strategies.

DISCUSSION

In this work, we describe a gene-drive system based on nickase versions of Cas9 that promotes super-Mendelian inheritance in *Drosophila*, and increases the number of feasible design options for gene-drives aimed at population engineering. We showed that both nD10A and nH840A produced efficient HDR in the germ line, but only when the two nicks in the DNA generated 5′ overhangs. We characterized events that failed to convert the wild-type allele to the gene-drive by Sanger sequencing, which indicated that nH840A combined with PAM-in gRNAs produced higher rates of large deletions compared to the nD10A and PAM-out arrangement. While the PAM-out condition triggered large insertions, we did not observe these alterations when we analyzed resistant alleles produced by the nH840A, which suggested that the modes of DNA repair that are triggered are nickase dependent.

In our experiments, nD10A produced higher super-Mendelian rates than nH840A, which we attributed to differences in cleavage activities between the nickases. In fact, nH840A has been shown to present less cleavage activity *in vitro* as it produced lower indel rates when disrupting the *EMX-S1* gene (Gopalappa et al., 2018). In addition, the distinct time windows of cleavage between the pairs of gRNAs, which need to cut simultaneously, may affect HDR efficiencies as both nickases showed super-Mendelian inheritance with different paired gRNAs. While previous studies did not report meaningful HDR rates with nH840A (Bothmer et al., 2017; Mali et al., 2013; Ran et al., 2013), we showed efficient HDR rates achieved by gRNAs in a PAM-in configuration when generating 5′ overhangs using nH840A for the first time. Thus, nH840A could be a viable option for future nickase-based designs to promote HDR.

While the focus of this work was to obtain a proof-of-concept for a Cas9-nickase gene-drive, we observed slightly higher super-Mendelian rates in the wild-type Cas9 over the nickases. We believe that this is because a nickase requires the coordinated action of both gRNAs cutting simultaneously to induce efficient HDR. Conversely, when the wild-type Cas9 is used, a single cut from either of the paired gRNAs can induce HDR to produce double-stranded DNA breaks. Furthermore, while the failure of the first gRNA would result in a small indel, the second gRNA can still cut and trigger a second round of potential conversion, which could explain the higher inheritance rates in the wild-type Cas9 scenario. Thus, it is imperative to thoroughly test the paired gRNAs to maximize coordinated action in future nickase gene-drive systems.

With regard to resistant allele formation, we have shown that our nH840A transgene combined with paired gRNAs in a PAM-in configuration frequently generated large deletions between the spaced nicks, which we did not detect when using gRNAs in a PAM-out configuration with nD10A. We could harness this effect to boost gene-drive propagation when specifically targeting essential genes. For example, the gene-drive element can carry a DNA rescue sequence to replace a wild-type allele while restoring the functionality of

vital genes to ensure animal viability and gene-drive spread. If resistant alleles occur from unsuccessful allelic conversion, then these mutations should produce nonviable animals that evade propagation, although small mutations in essential genes can still produce some viable escapees (Terradas et al., 2021). Therefore, large deletions induced by a gene-drive system using nH840A in a PAM-in configuration should help remove surviving escapees in a population carrying small indels.

We questioned whether a nickase gene-drive system could reduce the formation of resistant alleles, as DNA nicks are usually repaired efficiently. Indeed, we observed wild-type/uncut alleles within our nickase experiment conditions promoting biased inheritance, and this could help reduce resistant alleles formation while facilitating further gene drive conversion. However, we also detected resistant alleles caused by single DNA nicks, which could be from non-repaired single nicks that were converted to double-strand breaks that were subsequently fixed by non-homologous end-joining (Kuzminov, 2001). Importantly, mutations produced at a single target site by DNA nicks could limit further gene-drive propagation, as single nicks are poor HDR inducers (Vriend et al., 2016), and a single mutation at one target site would be enough to avoid gene-drive spread. However, our proposed nickase system is amenable to further optimization, especially as one major contributing factor to this may be due to fixing the induced DNA paired nicks to ~50 nt apart, although in fact, efficient HDR has been observed with offset distances ranging from 20 to 100 bp (Vriend et al., 2016). Thus, we envision further adapting our strategy in the future to generate distinct offset distances to improve the HDR efficiency of our nickase-based system.

Future nickase-gene-drive approaches could explore additional optimizations to increase specificity and reduce off-target effects, which can accumulate in a population and must be considered. As two independent cleavage events need to be coordinated for the desired modification, paired nicks were shown in previous work to improve specificity while reducing off-target effects when disrupting the *EMX1* gene in human cell culture (Ran et al., 2013). Recently, the off-target effects of gene-drives were predicted using validated algorithms and posterior *in vivo*-targeted deep sequencing with *Anopheles* mosquitoes in laboratory cage studies (Carballar-Lejarazú et al., 2020; Garrood et al., 2021). The off-targets effects were almost undetectable if using promoters that restricted Cas9 expression to the germline. Indeed, a nickase gene-drive system could be tested in *Anopheles* and species with much larger genomes, such as *Aedes* or *Culex* mosquitoes (Main et al., 2021; Severson et al., 2004), to study the pervasiveness of off-target effects across genome sizes and in the wild. Furthermore, gene-drives can bias Mendelian inheritance in mice (Grunwald et al., 2019; Weitzel et al., 2021). In the future, a nickase-based gene-drive system could also be applied to mice or to reduce off-target effects when editing mammalian embryos (Aryal et al., 2018).

Altogether, our proof-of-principle study provides a step toward the development of next-generation nickase-based gene drives that advances their potential future applications. We envision that our work will spur the use of nickase-based gene-drive systems for improved population control while encouraging its implementation in a broader range of organisms.

Limitations of the study

The nickase gene drive presented here utilized paired-gRNAs that are 50 nucleotides apart (offset distance). These gRNAs introduced DNA nicks and only promoted super-Mendelian inheritance when 5′ overhangs were generated. Although we observed high DNA HDR rates, the engineered cassette also generated undesired mutations in the germ line. Therefore, future experiments modifying the offset distance between gRNAs could help improve HDR rates while reducing the formation of mutations.

Nickase versions of Cas9 have been widely used in cell culture, yet nickases have not been extensively used in insects to promote HDR. Our proof-of-concept nickase gene-drive system represents an initial step, and its applicability for potential field interventions in insect pests such as mosquitoes still needs to be explored.

STAR★METHODS

RESOURCE AVAILABILITY

Lead contact—Any request will be fulfilled by the Lead Contact, Víctor López del Amo (vlopezdelamo@ucsd.edu).

Materials availability—Reagents generated in this work are available upon request and should be directed to the Lead contact. All reagents require a completed Materials Transfer Agreement.

Data and code availability

- Original raw counting data from the gene-drive experiments is provided as supplemental information.
- This work does not include any datasets or code.
- Any additional information required to reanalyze the data presented in this work is available from the Lead contact upon request.

EXPERIMENTAL MODEL AND SUBJECT DETAILS

All flies were kept on standard food with a 12/12 hours day/night cycle. Fly stocks are kept at 18°C, and all experimental crosses were performed at 25°C. All flies were anesthetized during our experiments using CO_2. F_0 crosses from gene-drive experiments were made in pools of 3–6 virgin females crossed to 3–6 males. F_1 experiments were always made in single pairs to track editing events happening singularly in the germline. The F_2 progeny was scored as male or female and sorted for a fluorescent marker (DsRed and/or GFP) using a Leica M165 F2 Stereomicroscope with fluorescence as an indicator of transgene inheritance rates. All experiments were performed in a high-security ACL2 (Arthropod Containment Level 2) facility built for gene drive purposes in the Division of Biological Sciences at the University of California, San Diego. Crosses were made in polypropylene vials (Genesee Scientific Cat. #32–120), and all flies were frozen for 48 hours before being removed from the facility, autoclaved, and discarded as biohazardous waste.

METHOD DETAILS

Plasmid construction—DNA constructs were built using NEBuilder HiFi DNA Assembly Master Mix (New England BioLabs Cat. #E2621) and transformed into NEB 10-beta electrocompetent *E.coli* (New England BioLabs Cat. #3020). DNA was extracted using a Qiagen Plasmid Midi Kit (Qiagen Cat. #12143) and sequenced by Sanger sequencing at Genewiz. Primers used for cloning can be found in the Key resources table below.

Transgenic line generation and genotyping—We outsourced embryo injections to Rainbow Transgenic Flies, Inc. All DNA constructs were injected into our lab's isogenized Oregon-R (Or-R) strain to ensure consistent genetic background throughout experiments. Plasmid templates were co-injected with a Cas9-expressing plasmid (pBSHsp70-Cas9 was a gift from Melissa Harrison & Kate O'Connor-Giles & Jill Wildonger [Addgene plasmid #46294; http://n2t.net/addgene:46294; RRID: Addgene_46294]). We received the injected generation 0 (G_0) animals, then we intercrossed the hatched adults in small pools (3–5 males × 3–5 females), and screened the G_1 flies for a fluorescent marker (DsRed for Cas9 versions and GFP for gene-drive elements, both fluorescences in the eye), which was indicative of transgene insertion. Lastly, we established homozygous lines from single transformants by crossing to Or-R. As the Cas9 transgene is inserted into the *yellow* gene disrupting it, homozygous flies for the Cas9 versions can be identified once flies display a yellow body color. Similarly for the Copycat constructs that are integrated into the *white* gene, homozygous flies for the CopyCat elements display a white eye phenotype. Stocks were sequenced by PCR and Sanger sequencing to confirm proper transgene insertion.

DNA extraction from single flies—To sequence resistant alleles, we extracted genomic DNA from individual males following the method described by Gloor GB and colleagues (Gloor et al., 1993). In brief, we used 50ul of the extraction buffer to squish single flies in a PCR tube. Next, we placed them into the PCR machine (Proflex PCR system, *Applied Biosystems*) for 1 hour at 37°C followed by 5 minutes at 95°C to inactivate the proteinase K. Then, we added to each DNA sample 200uL of water to obtain a total of 250uL per sample. Lastly, we used 1–5uL in a 25uL PCR reaction covering the gRNA cut sites in the *white* gene for Sanger sequencing analysis.

Sanger sequencing of individuals carrying resistance alleles—We amplified a DNA region covering the gRNA cut sites using the v1564 and v1565 oligos (see oligos list below). The obtained amplicon was then sequenced by Sanger sequencing to determine the quality of the resistant alleles using the v478 oligo. When we obtained lower-quality traces, we performed a second Sanger sequencing reaction from the other side of the amplicon to confirm the quality of the mutation with either the v659 or v1571 primers. Primers used for resistance allele sequencing can be found in the Key resources table.

Microscopy—Adult flies were anesthetized using CO2 to select individuals for crossing experiments. Their phenotypes were analyzed using a Leica M165 FC Stereo microscope to properly prepare the experimental crosses. Inheritance analysis of the transgenes marked with fluorescence was evaluated using the same microscope. DsRed marker implies presence of the Cas9 cassettes while GFP fluorescence indicates presence of the CopyCat transgenes.

QUANTIFICATION AND STATISTICAL ANALYSIS

We used GraphPad Prism 9 and Adobe Illustrator to generate all the graphs. Statistical analyses were performed using GraphPad Prism 9. In Figure 2B, we applied an unpaired *t test* to compare inheritance rates when using the wildtype Cas9 (Table S1). Additionally, One-Way Anova and Tukey's multiple comparison test to evaluate differences between super-Mendelian rates in our nickase gene-drive experiments in Figure 2C (Table S2). For evaluating the differences in proportions for resistant allele events in Figure 2E, we used Fisher's exact test (Table S3).

Supplementary Material

Refer to Web version on PubMed Central for supplementary material.

ACKNOWLEDGMENTS

We thank Kaycie Butler and JingXin Liang for comments and edits on the manuscript. The research reported in this manuscript was supported by the University of California, San Diego, Department of Biological Sciences, the Office of the Director of the National Institutes of Health under award no. DP5OD023098 (to V.M.G.), and the National Institute of Allergy and Infectious Diseases under award no. R01AI162911 (to V.M.G.). V.L.D.A. and V.M.G. are authors on a patent filed by the University of California, San Diego (provisional application serial no. 63/254,753) that is related to the nickase gene-drive system described in this work.

REFERENCES

Adolfi A, Gantz VM, Jasinskiene N, Lee H-F, Hwang K, Terradas G, Bulger EA, Ramaiah A, Bennett JB, Emerson JJ, et al. (2020). Efficient population modification gene-drive rescue system in the malaria mosquito Anopheles stephensi. Nat. Commun 11, 5553. 10.1038/s41467-020-19426-0. [PubMed: 33144570]

Aryal NK, Wasylishen AR, and Lozano G (2018). CRISPR/Cas9 can mediate high-efficiency off-target mutations in mice in vivo. Cell Death Dis. 9, 1099. 10.1038/s41419-018-1146-0. [PubMed: 30368519]

Bier E (2021). Gene drives gaining speed. Nat. Rev. Genet 23, 5–22. 10.1038/s41576-021-00386-0. [PubMed: 34363067]

Bothmer A, Phadke T, Barrera LA, Margulies CM, Lee CS, Buquicchio F, Moss S, Abdulkerim HS, Selleck W, Jayaram H, et al. (2017). Characterization of the interplay between DNA repair and CRISPR/Cas9-induced DNA lesions at an endogenous locus. Nat. Commun 8, 13905. 10.1038/ncomms13905. [PubMed: 28067217]

Caldecott KW (2008). Single-strand break repair and genetic disease. Nat. Rev. Genet 9, 619–631. 10.1038/nrg2380. [PubMed: 18626472]

Carballar-Lejarazú R, Ogaugwu C, Tushar T, Kelsey A, Pham TB, Murphy J, Schmidt H, Lee Y, Lanzaro GC, and James AA (2020). Next-generation gene drive for population modification of the malaria vector mosquito, Anopheles gambiae. Proc. Natl. Acad. Sci. U S A 117, 22805–22814. 10.1073/pnas.2010214117. [PubMed: 32839345]

Chafin DR, Vitolo JM, Henricksen LA, Bambara RA, and Hayes JJ (2000). Human DNA ligase I efficiently seals nicks in nucleosomes. EMBO J. 19, 5492–5501. 10.1093/emboj/19.20.5492. [PubMed: 11032816]

Champer J, Liu J, Oh SY, Reeves R, Luthra A, Oakes N, Clark AG, and Messer PW (2018). Reducing resistance allele formation in CRISPR gene drive. Proc. Natl. Acad. Sci. U S A 115, 5522–5527. 10.1073/pnas.1720354115. [PubMed: 29735716]

Champer J, Chung J, Lee YL, Liu C, Yang E, Wen Z, Clark AG, and Messer PW (2019). Molecular safeguarding of CRISPR gene drive experiments. Elife 8, e41439. 10.7554/elife.41439. [PubMed: 30666960]

Gantz VM, and Bier E (2015). The mutagenic chain reaction: a method for converting heterozygous to homozygous mutations. Science 348, 442–444. 10.1126/science.aaa5945. [PubMed: 25908821]

Gantz VM, and Bier E (2016). The dawn of active genetics. Bioessays 38, 50–63. 10.1002/bies.201500102. [PubMed: 26660392]

Gantz VM, Jasinskiene N, Tatarenkova O, Fazekas A, Macias VM, Bier E, and James AA (2015). Highly efficient Cas9-mediated gene drive for population modification of the malaria vector mosquito Anopheles stephensi. Proc. Natl. Acad. Sci. U S A 112, E6736–E6743. 10.1073/pnas.1521077112. [PubMed: 26598698]

Garrood WT, Kranjc N, Petri K, Kim DY, Guo JA, Hammond AM, Morianou I, Pattanayak V, Joung JK, Crisanti A, and Simoni A (2021). Analysis of off-target effects in CRISPR-based gene drives in the human malaria mosquito. Proc. Natl. Acad. Sci. U S A 118, e2004838117. 10.1073/pnas.2004838117. [PubMed: 34050017]

Gasiunas G, Barrangou R, Horvath P, and Siksnys V (2012). Cas9-crRNA ribonucleoprotein complex mediates specific DNA cleavage for adaptive immunity in bacteria. Proc. Natl. Acad. Sci. U S A 109, E2579–E2586. 10.1073/pnas.1208507109. [PubMed: 22949671]

Gloor GB, Preston CR, Johnson-Schlitz DM, Nassif NA, Phillis RW, Benz WK, Robertson HM, and Engels WR (1993). Type I repressors of P element mobility. Genetics 135, 81–95. 10.1093/genetics/135.1.81. [PubMed: 8224830]

Gopalappa R, Suresh B, Ramakrishna S, and Kim HH (2018). Paired D10A Cas9 nickases are sometimes more efficient than individual nucleases for gene disruption. Nucleic Acids Res. 46, e71. 10.1093/nar/gky222. [PubMed: 29584876]

Grunwald HA, Gantz VM, Poplawski G, Xu X-RS, Bier E, and Cooper KL (2019). Super-Mendelian inheritance mediated by CRISPR-Cas9 in the female mouse germline. Nature 566, 105–109. 10.1038/s41586-019-0875-2. [PubMed: 30675057]

Hammond A, Galizi R, Kyrou K, Simoni A, Siniscalchi C, Katsanos D, Gribble M, Baker D, Marois E, Russell S, et al. (2016). A CRISPR-Cas9 gene drive system targeting female reproduction in the malaria mosquito vector Anopheles gambiae. Nat. Biotechnol 34, 78–83. 10.1038/nbt.3439. [PubMed: 26641531]

Hammond AM, Kyrou K, Bruttini M, North A, Galizi R, Karlsson X, Kranjc N, Carpi FM, D'Aurizio R, Crisanti A, and Nolan T (2017). The creation and selection of mutations resistant to a gene drive over multiple generations in the malaria mosquito. PLoS Genet. 13, e1007039. 10.1371/journal.pgen.1007039. [PubMed: 28976972]

Hyodo T, Rahman ML, Karnan S, Ito T, Toyoda A, Ota A, Wahiduzzaman M, Tsuzuki S, Okada Y, Hosokawa Y, and Konishi H (2020). Tandem paired nicking promotes Precise genome editing with scarce interference by p53. Cell Rep. 30, 1195–1207.e7. 10.1016/j.celrep.2019.12.064. [PubMed: 31995758]

Jinek M, Chylinski K, Fonfara I, Hauer M, Doudna JA, and Charpentier E (2012). A programmable dual-RNA-guided DNA endonuclease in adaptive bacterial immunity. Science 337, 816–821. 10.1126/science.1225829. [PubMed: 22745249]

Kuzminov A (2001). Single-strand interruptions in replicating chromosomes cause double-strand breaks. Proc. Natl. Acad. Sci. U S A 98, 8241–8246. 10.1073/pnas.131009198. [PubMed: 11459959]

Kyrou K, Hammond AM, Galizi R, Kranjc N, Burt A, Beaghton AK, Nolan T, and Crisanti A (2018). A CRISPR-Cas9 gene drive targeting doublesex causes complete population suppression in caged Anopheles gambiae mosquitoes. Nat. Biotechnol 36, 1062–1066. 10.1038/nbt.4245. [PubMed: 30247490]

Lee AY, and Lloyd KC (2014). Conditional targeting of Ispd using paired Cas9 nickase and a single DNA template in mice. FEBS Open Bio 4, 637–642.

Li M, Yang T, Kandul NP, Bui M, Gamez S, Raban R, Bennett J, Sánchez C HM, Lanzaro GC, Schmidt H, et al. (2020). Development of a confinable gene drive system in the human disease vector Aedes aegypti. Elife 9, e51701. 10.7554/elife.51701. [PubMed: 31960794]

López Del Amo V, Leger BS, Cox KJ, Gill S, Bishop AL, Scanlon GD, Walker JA, Gantz VM, and Choudhary A (2020a). Small-molecule control of super-mendelian inheritance in gene drives. Cell Rep. 31, 107841. 10.1016/j.celrep.2020.107841. [PubMed: 32610142]

Ló pez Del Amo V, Bishop AL, Sánchez CHM, Bennett JB, Feng X, Marshall JM, Bier E, and Gantz VM (2020b). A transcomplementing gene drive provides a flexible platform for laboratory investigation and potential field deployment. Nat. Commun 11, 352. 10.1038/s41467-019-13977-7. [PubMed: 31953404]

Main BJ, Marcantonio M, Johnston JS, Rasgon JL, Brown CT, and Barker CM (2021). Whole-genome assembly of Culex tarsalis. G3 11, jkaa063. [PubMed: 33585869]

Mali P, Aach J, Stranges PB, Esvelt KM, Moosburner M, Kosuri S, Yang L, and Church GM (2013). CAS9 transcriptional activators for target specificity screening and paired nickases for cooperative genome engineering. Nat. Biotechnol 31, 833–838. 10.1038/nbt.2675. [PubMed: 23907171]

Port F, Chen H-M, Lee T, and Bullock SL (2014). Optimized CRISPR/Cas tools for efficient germline and somatic genome engineering in Drosophila. Proc. Natl. Acad. Sci. U S A 111, E2967–E2976. 10.1073/pnas.1405500111. [PubMed: 25002478]

Ran FA, Hsu PD, Lin C-Y, Gootenberg JS, Konermann S, Trevino AE, Scott DA, Inoue A, Matoba S, Zhang Y, and Zhang F (2013). Double nicking by RNA-guided CRISPR Cas9 for enhanced genome editing specificity. Cell 155, 479–480. 10.1016/j.cell.2013.09.040.

Ren X, Yang Z, Mao D, Chang Z, Qiao HH, Wang X, Sun J, Hu Q, Cui Y, Liu LP, Ji JY, Xu J, and Ni JQ (2014). Performance of the Cas9 nickase system in Drosophila melanogaster. G3 (Bethesda) 4, 1955–1962. [PubMed: 25128437]

Reyes GX, Kolodziejczak A, Devakumar LJPS, Kubota T, Kolodner RD, Putnam CD, and Hombauer H (2021). Ligation of newly replicated DNA controls the timing of DNA mismatch repair. Curr. Biol 31, 1268–1276.e6. 10.1016/j.cub.2020.12.018. [PubMed: 33417883]

Severson DW, DeBruyn B, Lovin DD, Brown SE, Knudson DL, and Morlais I (2004). Comparative genome analysis of the yellow fever mosquito Aedes aegypti with Drosophila melanogaster and the malaria vector mosquito Anopheles gambiae. J. Hered 95, 103–113. 10.1093/jhered/esh023. [PubMed: 15073225]

Simoni A, Hammond AM, Beaghton AK, Galizi R, Taxiarchi C, Kyrou K, Meacci D, Gribble M, Morselli G, Burt A, et al. (2020). A male-biased sex-distorter gene drive for the human malaria vector Anopheles gambiae. Nat. Biotechnol 38, 1054–1060. 10.1038/s41587-020-0508-1. [PubMed: 32393821]

Terradas G, Buchman AB, Bennett JB, Shriner I, Marshall JM, Akbari OS, and Bier E (2021). Inherently confinable split-drive systems in Drosophila. Nat. Commun 12, 1480. 10.1038/s41467-021-21771-7. [PubMed: 33674604]

Vriend LEM, and Krawczyk PM (2017). Nick-initiated homologous recombination: Protecting the genome, one strand at a time. DNA Repair 50, 1–13. 10.1016/j.dnarep.2016.12.005. [PubMed: 28087249]

Vriend LEM, Prakash R, Chen C-C, Vanoli F, Cavallo F, Zhang Y, Jasin M, and Krawczyk PM (2016). Distinct genetic control of homologous recombination repair of Cas9-induced double-strand breaks, nicks and paired nicks. Nucleic Acids Res. 44, 5204–5217. 10.1093/nar/gkw179. [PubMed: 27001513]

Wang H, and Hays JB (2007). Human DNA mismatch repair: coupling of mismatch recognition to strand-specific excision. Nucleic Acids Res. 35, 6727–6739. 10.1093/nar/gkm734. [PubMed: 17921148]

Wang Q, Liu J, Janssen JM, Le Bouteiller M, Frock RL, and Gonçalves MAFV (2021). Precise and broad scope genome editing based on high-specificity Cas9 nickases. Nucleic Acids Res. 49, 1173–1198. 10.1093/nar/gkaa1236. [PubMed: 33398349]

Wang Y, Zhao J, Duan N, Liu W, Zhang Y, Zhou M, Hu Z, Feng M, Liu X, Wu L, et al. (2018). Paired CRISPR/Cas9 nickases mediate efficient site-specific integration of F9 into rDNA locus of mouse ESCs. Int. J. Mol. Sci 19, 3035. 10.3390/ijms19103035.

Weitzel AJ, Grunwald HA, Levina R, Gantz VM, Hedrick SM, Bier E, and Cooper KL (2021). Meiotic Cas9 expression mediates genotype conversion in the male and female mouse germline. Preprint at bioRxiv. 10.1101/2021.03.16.435716.

Xu X-RS, Gantz VM, Siomava N, and Bier E (2017). CRISPR/Cas9 and active genetics-based trans-species replacement of the endogenous Drosophila kni-L2 CRM reveals unexpected complexity. Elife 6, e30281. 10.7554/elife.30281. [PubMed: 29274230]

Highlights

- Nickase versions of Cas9 trigger DNA homology-directed (HDR) repair *in vivo*
- Paired DNA nicks into DNA promote gene-drive's super-Mendelian inheritance
- Efficient gene-drive propagation occurs when 5′ overhangs are generated
- Nickase genedrive-producing 3′ overhangs do not trigger HDR

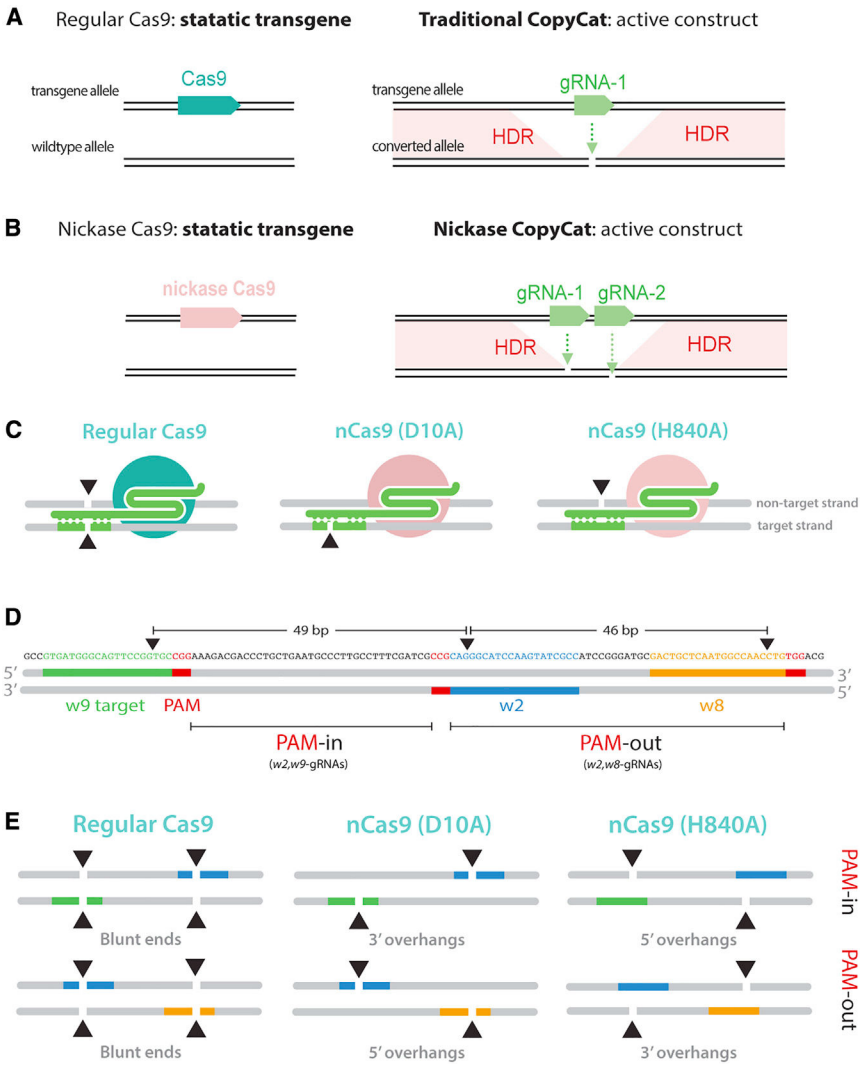

Figure 1. A nickase-based gene-drive system promotes different overhang patterns

(A) Schematic diagram of a traditional CopyCat gene-drive system. When combined with a Cas9 source, the gRNA cassette replaces the wild-type allele (converted allele) by DNA double-strand break and subsequent homology directed-repair (HDR).

(B) A nickase Cas9 source is combined with a Copycat containing 2 gRNAs targeting each complementary strand of the wild-type allele to spread the paired gRNA cassette by HDR.

(C) Wild-type Cas9 cuts both DNA strands, nD10A cuts the target strand where the gRNA is bound, and nH840 cuts the non-target strand.

(D) Sequence and design of the paired gRNAs in both PAM-out and PAM-in orientation. Paired gRNAs target sites are located ~50 nt apart. The depicted gRNAs bind to the opposite strand when produced by complementarity. Red boxes indicate the PAM sequences (not included in the gRNA) that are crucial for DNA recognition. The black triangles denote the different cut sites associated with each gRNA.

(E) Wild-type Cas9 introduces blunt ends when combined with either of the CopyCat elements. nD10A and nH840, combined with paired gRNAs binding to specific DNA

strands, can generate 5′ or 3′ overhangs as they target different strands (target and non-target strands, respectively).

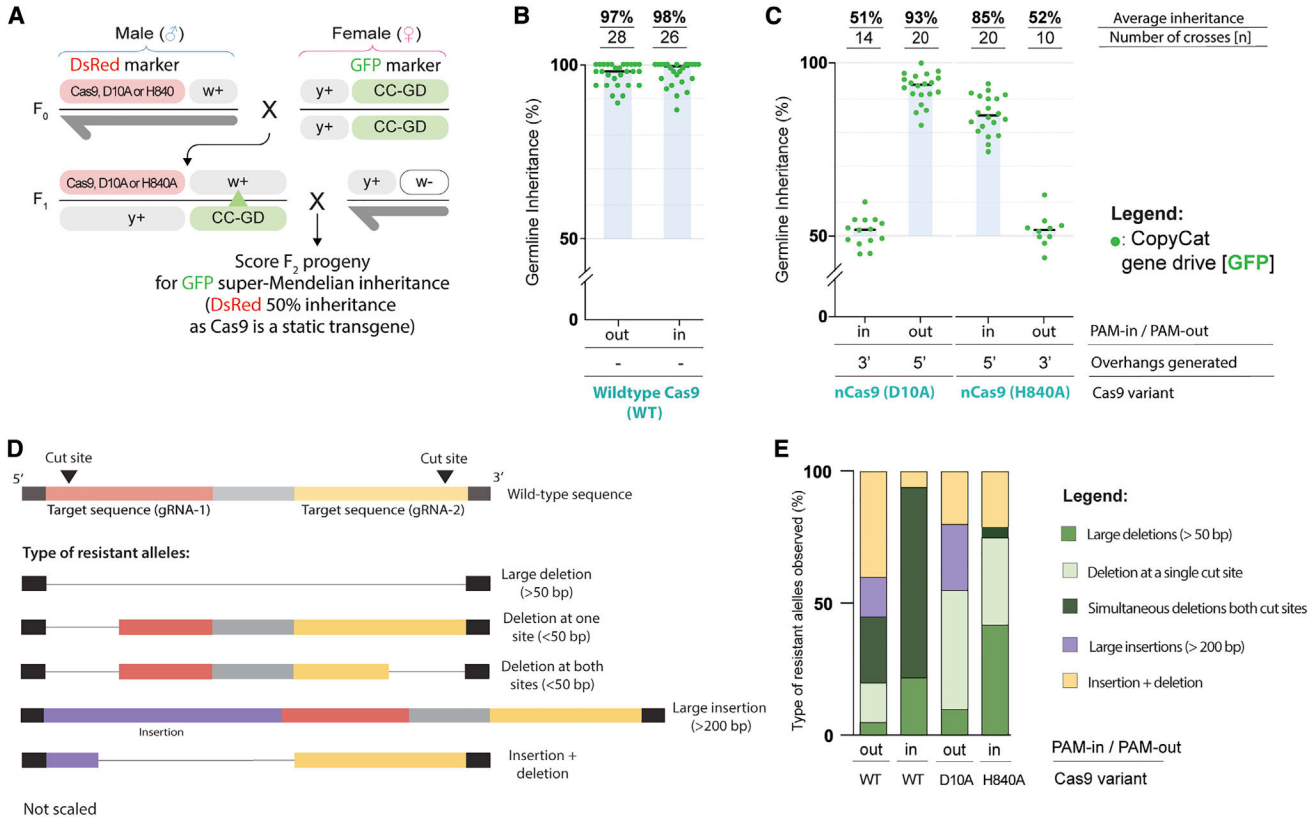

Figure 2. Super-Mendelian inheritance rates produced by nickase Cas9s when 5′ overhangs are generated

(A) All Cas9 sources (wild-type Cas9, nD10A, and nH840A) and the CopyCat elements are inserted in the X chromosome (*yellow* [y] and *white* [w] genes, respectively). F0 males containing the Cas9 were crossed to females containing either Copycat gene-drives (CC-GD). F1 females carrying both transgenes were crossed to wild-type males to assess germline allelic conversion (green triangle indicates potential wild-type allele replacement) by scoring the GFP marker in the F2.

(B) Similar biased inheritance rates were observed when wild-type Cas9 was combined with both CopyCat elements.

(C) nD10A and nH840A triggered super-Mendelian inheritance rates only when generating 5′ overhangs.

(D) Schematic of observed resistant allele outcomes in the gene-drive experiments.

(E) Cas9 PAM-out (n = 20) displayed large insertions while Cas9 PAM-in (n = 18) produced high rates of simultaneous mutations occurring at both target sites. nD10A (n = 20) produced a high frequency of large insertions, while nH840A (n = 24) produced bigger deletions between nick sites.

KEY RESOURCES TABLE

REAGENT or RESOURCE	SOURCE	IDENTIFIER
Experimental models: Organisms/strains		
D. mel: Wildtype Cas9	This work	N/A
D. mel: Nickase D10A Cas9	This work	N/A
D. mel: Nickase H840A Cas9	This work	N/A
D. mel: Gene-drive CopyCat (w2-w8 gRNAs)	This work	N/A
D. mel: Gene-drive CopyCat (w2-w9 gRNAs)	This work	N/A
Oligonucleotides		
See Table S4 for the Primers used in the study	This paper	N/A
Recombinant DNA		
Plasmid (p): *vasa*-wildtype Cas9	This work	N/A
Plasmid (p): *vasa*-nickase D10A Cas9	This work	N/A
Plasmid (p): *vasa*-nickase H840A Cas9	This work	N/A
Plasmid (p): U6:1_w2-gRNA U6:3_w8-gRNA	This work	N/A
Plasmid (p): U6:1_w2-gRNA U6:3_w9-gRNA	This work	N/A